We are IntechOpen, the world's leading publisher of Open Access books Built by scientists, for scientists

4,800
Open access books available

122,000
International authors and editors

135M
Downloads

Our authors are among the

154
Countries delivered to

TOP 1%
most cited scientists

12.2%
Contributors from top 500 universities

CLARIVATE ANALYTICS BOOK CITATION INDEX INDEXED

WEB OF SCIENCE™

Selection of our books indexed in the Book Citation Index in Web of Science™ Core Collection (BKCI)

Interested in publishing with us?
Contact book.department@intechopen.com

Numbers displayed above are based on latest data collected.
For more information visit www.intechopen.com

25

Pulse Wave Propagation in Bistable Oscillator Array

Kuniyasu Shimizu[1], Motomasa Komuro[2] and Tetsuro Endo[3]
[1]*Chiba Institute of Technology*
[2]*Teikyo University of Science and Technology*
[3]*Meiji University*
Japan

1. Introduction

A study of propagating wave phenomenon in coupled systems is one of the familiar topics of research. There exist propagating wave phenomena in various systems such as reaction-diffusion systems (Nishiura et al.; 2005; Comte et al.; 2001), coupled map lattice (Kaneko; 1993) and coupled oscillator systems (Hikihara et al.; 2001; Yamauchi et al.; 1999), etc.. They are important not only in a pure nonlinear science viewpoint but also from the viewpoint of various applications such as engineering purpose (Sato et al.; 2003) and biological information processing (Keener; 1987). A basic question concerning these systems is the condition under which propagating wave can emerge. It is known as propagation failure phenomenon that propagating wave fails to propagate below a certain critical coupling strength (Comte et al.; 2001).

In this chapter, a simple model of one-dimensinally coupled bistable oscillators is shown to exhibit wave propagation phenomena. The propagating wave consists of several adjacent oscillators oscillating with large amplitude, and the part of large amplitude oscillation in the array propagates with a constant speed. In particular, we pay attention to the formation mechanism of the propagating wave related to disappearance of a certain kind of standing wave. When a coupling strength is weak, a standing pulse wave exists. This solution disappears when the coupling strength exceeds a certain critical value, and around this point the propagating wave begins to exist. On the basis of the observation, one of the onset mechanisms of the propagating waves is investigated paying attention to global phase-space structure around the bifurcation point.

At first, we will introduce the ring of coupled bistable oscillator system, and derive the fundamental equation. Then, a typical propagating wave phenomenon and its characteristic features are stated briefly. Next, we make a study on the onset mechanism of the propagating wave for 6 coupled oscillator case. As a result, we have found that a global bifurcation of maps based on the heteroclinic tangle converts the fixed point (= standing wave) into the invariant circle (= propagating pulse wave).

Source: Wave Propagation in Materials for Modern Applications, Book edited by: Andrey Petrin,
ISBN 978-953-7619-65-7, pp. 526, January 2010, INTECH, Croatia, downloaded from SCIYO.COM

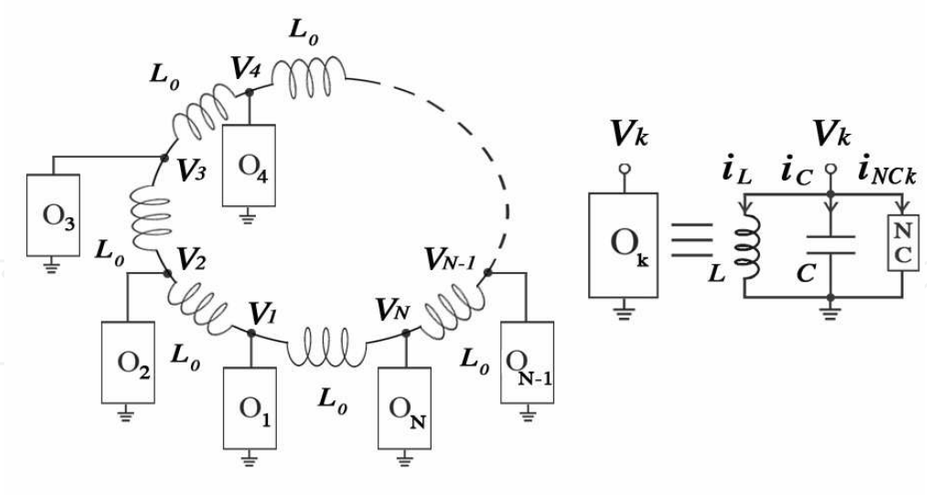

(a) A ring of N-coupled bistable oscillators

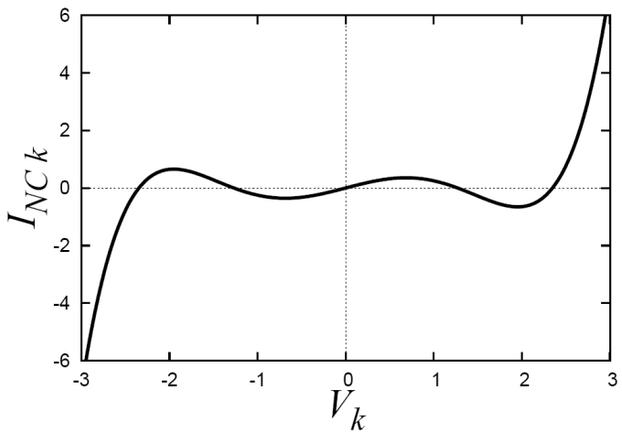

(b) The fifth-power nonlinearity on the I-V characteristics of NC

Fig. 1. A circuit model

2. Fundamental equation and its dynamics

Figure 1(a) shows a circuit model of the ring of N-coupled bistable oscillators. The current-voltage characteristics of negative conductance (= NC) in Fig.1(a) has the fifth-power nonlinearity as shown in Fig.1(b): $i_{NCk} = g_1 V_k - g_3 V_k^3 + g_5 V_k^5$, $g1$, $g3$, $g5 > 0$, $k = 1, 2, \ldots, N$. Then, Kirchhoff's current law gives the following equation:

$$\frac{1}{L}\int V_k dt + C\frac{dV_k}{dt} + g_1 V_k - g_3 V_k^3 + g_5 V_k^5 = \frac{1}{L_0}\int (V_{k-1} - 2V_k + V_{k+1})dt, \quad k = 1,2,\cdots,N. \tag{1}$$

Taking time derivative of (1), we obtain the following equation (V_0 [resp. V_{N+1}] is regarded as V_N [resp. V_1]).

$$\frac{d^2V_k}{dt^2}+\frac{g_1}{C}(1-\frac{3g_3}{g_1}V_k^2+\frac{5g_5}{g_1}V_k^4)\frac{dV_k}{dt}+\left(\frac{1}{LC}+\frac{2}{L_0C}\right)V_k-\frac{1}{L_0C}(V_{k-1}+V_{k+1})=0.$$

By normalizing the time and voltage variables:

$$t=\tau/\sqrt{(1/LC)+(1/L_0C)},\quad V_k=\sqrt[4]{g_1/5g_5}x_k,$$

and introducing new parameters:

$$\varepsilon\equiv g_1/\sqrt{(C/L)+(C/L_0)},\quad \alpha\equiv L/(L+L_0),$$

$$\beta\equiv 3g_3/\sqrt{5g_1g_5}.$$

the equation of this system can be written in the following normalized equation ($\cdot = d/d\tau$, $\cdot\cdot = d^2/d\tau^2$).

$$\ddot{x}_k+\varepsilon(1-\beta x_k^2+x_k^4)\dot{x}_k+(1-\alpha)x_k-\alpha(x_{k-1}-2x_k+x_{k+1})=0 \tag{2}$$

If we introduce new variables as $y_k \equiv \dot{x}_k$, we obtain the following autonomous ordinary differential equation.

$$\begin{aligned}\dot{x}_k&=y_k\\ \dot{y}_k&=-\varepsilon(1-\beta x_k^2+x_k^4)y_k\\ &\quad -(1-\alpha)x_k+\alpha(x_{k-1}-2x_k+x_{k+1})\end{aligned} \tag{3}$$

$$, k=1,2,\cdots,N,\quad x_0=x_N, x_1=x_{N+1},$$

, where N is the number of oscillators. The x_k denotes the normalized output voltage of the kth oscillator, y_k denotes its derivative. The parameter ε (> 0) shows the degree of nonlinearity. The parameter α ($0 \leqq \alpha \leqq 1$) is a coupling factor; namely α = 1 means maximum coupling, and α = 0 means no coupling. The parameter β controls amplitude of oscillation. Each isolated oscillator has two steady-states, namely, no oscillation and periodic oscillation depending on the initial condition.

The analysis of modes based on the averaging method or perturbation method for weakly nonlinear cases was extensively performed in the past (Endo & Ohta; 1980; Yoshinaga & Kawakami; 1993). However, the solution for non-weak nonlinear cases seems not to be analyzed; in fact, it is complicated including the propagating pulse wave solution. In this study, we analyze the onset mechanism of the propagating pulse wave solution for non-weak nonlinear case via bifurcation theory. The propagating pulse wave solution consists of several adjacent oscillators oscillating with large amplitude, and the part of large amplitude oscillation in the ring array propagates with a constant speed as shown in Fig.2[1].

This propagating pulse wave solution has the following characteristic features from the results in (Shimizu et al.; 2008).

[1] Numerical integrations throughout this paper are carried out by 4th order Runge-Kutta method with a step size of 0.01 if not otherwise specified.

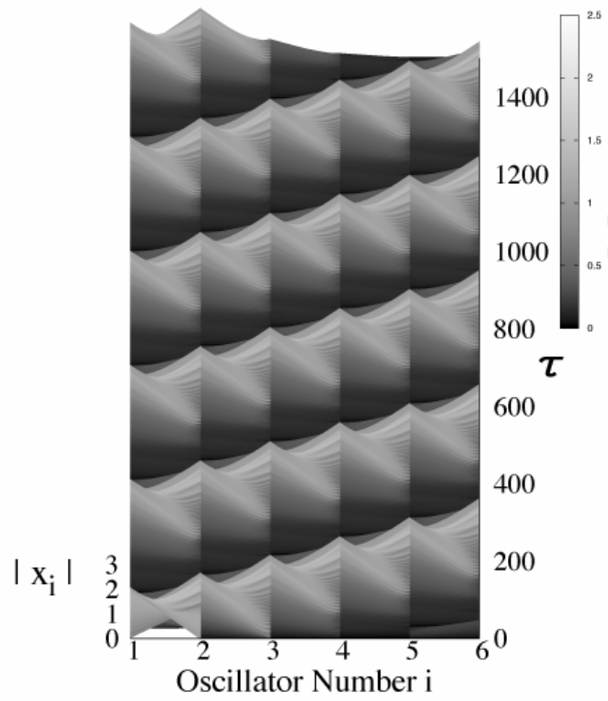

Fig. 2. A typical propagating pulse wave observed for the ring of 6 coupled oscillators (the absolute value of x-components are plotted for clarity). The initial condition is given as $x_1 = 2.0$, $y_2 = 1.3$ and all other variables are zero. ($\alpha = 0.1$, $\beta = 3.2$ and $\varepsilon = 0.36$)

- The direction of the propagating pulse wave depends on the initial condition.
- Propagating speed becomes faster for larger α.
- Robust against fluctuation and noise especially for comparatively large α.

Such propagating pulse wave seems to be observed for an arbitrary number of coupled oscillators[2] in comparatively large parameter regime. For instance, the existence region of several solutions including the propagating wave is shown in (Shimizu et al.; 2008) for the 100 coupled oscillator case by computer simulation. Hereafter, we will show one of the onset mechanisms of the propagating pulse wave for the ring of 6-coupled oscillators.

3. One of the onset mechanisms of propagating pulse wave

In this system, there exists a certain kind of standing pulse wave solution for small coupling strength α. The standing pulse wave solution is a periodic oscillation, one of which is shown in Fig.3. At first, we investigate this type of standing pulse wave, and then the transition from the standing pulse wave to the propagating pulse wave. Moreover, we will explain that the results obtained for the 6 coupled oscillator case may be extended to larger number of coupled oscillator cases.

[2] We confirmed the existence of the propagating pulse wave for the $N = 5$ to $N = 100$ cases via computer simulation.

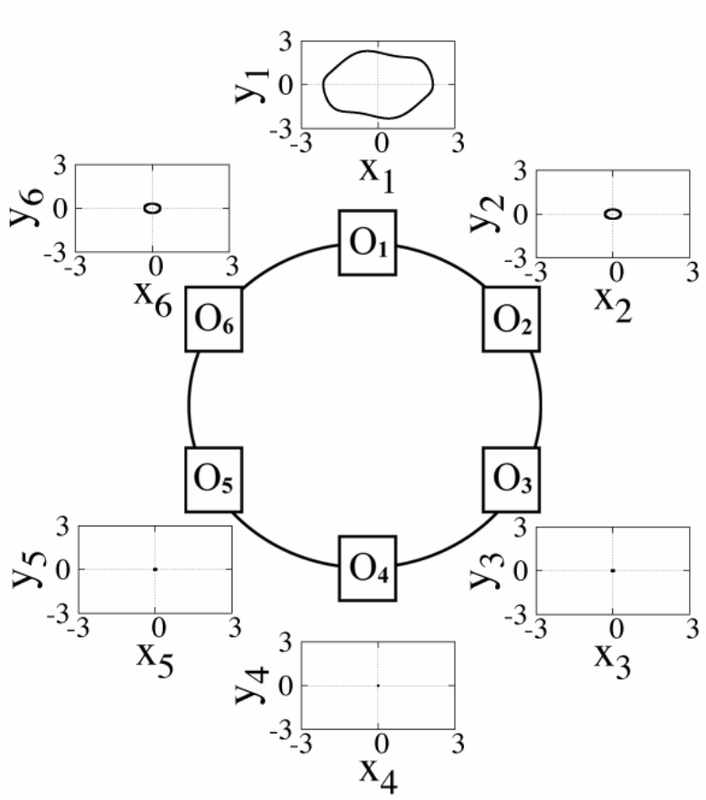

Fig. 3. A standing pulse wave (= a periodic solution) occurring in the ring of 6-coupled oscillators. Initial condition: $x_1(0) = 2.0$, $y_1(0) = 0.0$ and $x_k(0) = y_k(0) = 0.0$, $k = 2, 3, \ldots, 6$. Parameters: $\alpha = 0.05$, $\beta = 3.2$ and $\varepsilon = 0.36$.

3.1 The standing pulse wave

Figure 3 shows one of the periodic solutions (the standing pulse wave) obtained from the initial condition: $x_1(0) = 2.0$, $y_1(0) = 0.0$ and $x_k(0) = y_k(0) = 0$, $k = 2, 3, \ldots, 6$ for $\alpha = 0.05$, $\beta = 3.2$ and $\varepsilon = 0.36$. We choose $\alpha = 0.05$ in order to realize weak coupling so that there exists the standing pulse wave. Since this system has rotational symmetric property (due to ring coupling structure), other 5 periodic solutions obviously coexist for the same parameters. We define Poincare section as $y_1 = 0$[3], and trace these periodic solutions with respect to α (because the characteristic features of the propagating pulse wave mainly depends on coupling strength). Since the periodic solution becomes a fixed point on the Poincare section, this point becomes a curve when α is varied. In this manner, we can trace 6 periodic solutions as depicted in Fig.4 (Kawakami; 1984). The solid curves are mapped points corresponding to the above mentioned stable periodic solutions, namely the nodes (N_i, i = 1, 2, . . . , 6). The dotted curves represent their corresponding saddles ($\bar{S}_i$, i = 1, 2, . . . , 6)[4].

The node and the corresponding saddle coalesce at a certain value of α. This is called the Saddle-Node (SN) bifurcation point α_{SN}. In this system, there are 6 pairs of (N_i, S_i) curves

[3] We take mapped points when the flow penetrates the hyper-plane from + to –.

[4] This saddle is index 2, at least, for $\alpha \geqq 0.05$.

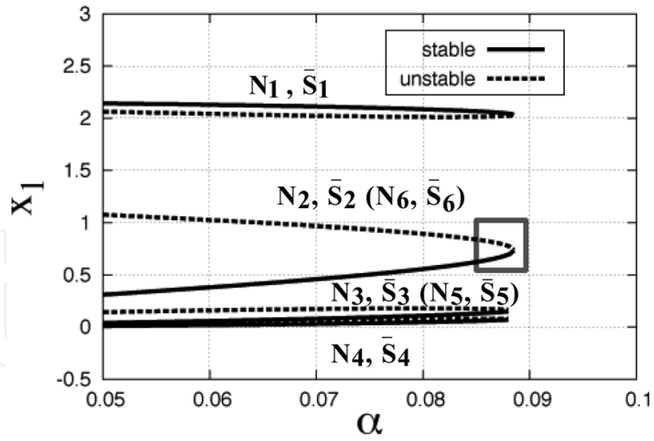

Fig. 4. The node Ni with its corresponding saddle $\bar{S}_i$ for i = 1, 2, ... , 6 showing the SN bifurcation in terms of α for β = 3.2 and ε = 0.36. The curve (N_2, $\bar{S}_2$) overlaps with the curve (N_6, $\bar{S}_6$), and (N_3, $\bar{S}_3$) with (N_5, $\bar{S}_5$), because they are symmetrically-placed. Subtle structure around the tip region surrounded by a square box is shown in Fig.6(a).

and they disappear simultaneously at the same SN bifurcation point. Namely, the aligned structure of the SN bifurcation points is formed at $\alpha_{SN} \doteqdot 0.088$ in this case. This is rough explanation of bifurcation diagram. In fact, the tip region of each curve presents more sophisticated bifurcations. This is explained later.

3.2 Propagating pulse wave based on the global bifurcation of maps

The SN bifurcation set of the periodic solution shown in Fig.3 and the existence regions of several solutions are depicted in Fig.5 in the α - β plane for ε = 0.36. Each solution is confirmed by direct computer simulation of (3). In the left hand side region of the SN bifurcation curve, there exist the 6 periodic solutions (abbr."PS" in Fig.5) and they disappear simultaneously at this SN bifurcation point approximately[5]. After the SN bifurcation, several types of solutions can be observed depending on the value of β. For instance, in the "W" region, the whole oscillation such as all oscillators oscillate with large amplitude can be observed. In the "Z" region, no oscillation exists. In the meantime, two different kinds of propagating pulse waves emerge. One of them ("PW1") is observed in the region filled with gray color. It should be noted that PW1 emerges right after the SN bifurcation for $3.14 \leqq \beta \leqq 3.25$. The other abbreviated as the "PW2" is shown with mesh pattern. The PW2 is different kind of propagating pulse wave from PW1 (A). In the following discussion, we focus on the dynamics of PW1 observed for $3.14 \leqq \beta \leqq 3.25$ and explain the onset mechanism of PW1 solution.

3.2.1 Global bifurcation related to the onset of PW1

For simplicity, we fix ε = 0.36 and β = 3.2. Figure 6 (a) presents the magnified bifurcation diagram in the square region of Fig.4. From this figure, it is noted that before the SN bifurcation a pitchfork bifurcation (PF) occurs. After the PF bifurcation, a stable node

[5] More accurately, the periodic solution disappears at α_{PF} in Fig.6(a). But, α_{PF} and α_{SN} are very close. So, we say the periodic solution disappears at α_{SN} approximately.

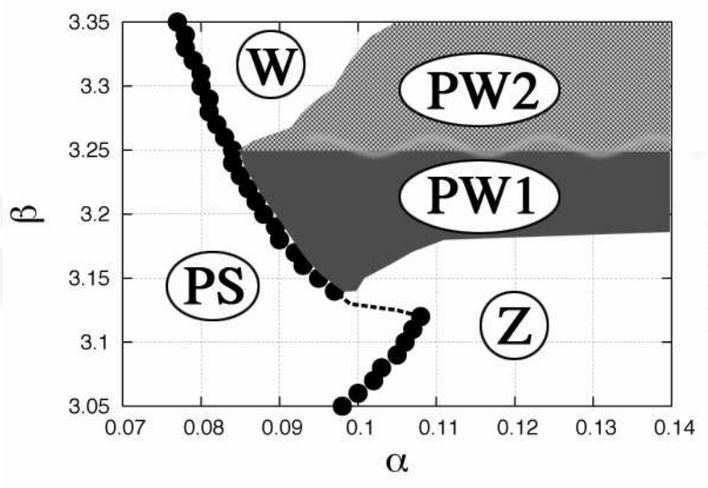

Fig. 5. The SN bifurcation set of the periodic solution in Fig.3 (black dots) and the existence regions of several solutions in the α - β plane for ε = 0.36. The "PS", "W" and "Z" are existence regions of the standing pulse wave, whole oscillation and no oscillation, respectively. In addition, there exist two kinds of propagating pulse waves. They are labeled as "PW1" and" PW2". For 3.12 < β < 3.14 (dotted curve), more complicated bifurcation phenomena including Neimark-Sacker bifurcation is detected, but this region is of no concern with our discussion from now on. In the boundary region, PW1 and PW2 coexist.

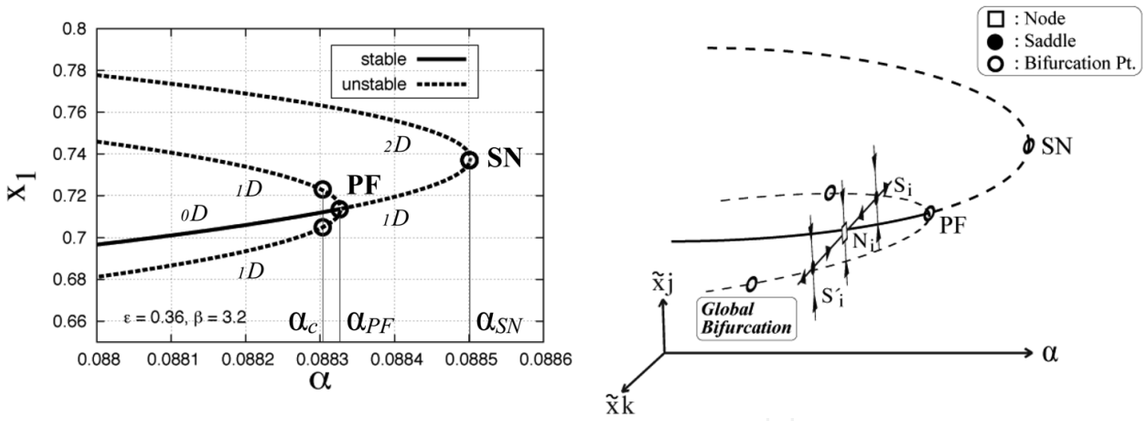

(a) Actual bifurcation diagram. (b) The 3D schematic diagram of (a)

Fig. 6. Subtle bifurcation diagram around the tip region surrounded by a square in Fig.4 for ε = 0.36 and β = 3.2. The bifurcation points are as follows: α_{SN} = 0.088501, α_{PF} = 0.088328 and α_c = 0.088302. The solid curve denotes stable and the dotted curve denotes unstable fixed point. (a) Actual bifurcation diagram. The notation ${}_mD$ indicates that number of unstable direction of the fixed point is "m". (b) 3D schematic diagram around the tip region. The axis $\tilde{x}_j$ denotes the stable direction of saddles and the axis $\tilde{x}_k$ unstable direction of them. The axes $\tilde{x}_j$ and $\tilde{x}_k$ may not correspond to the actual state variables x_j and x_k directly.

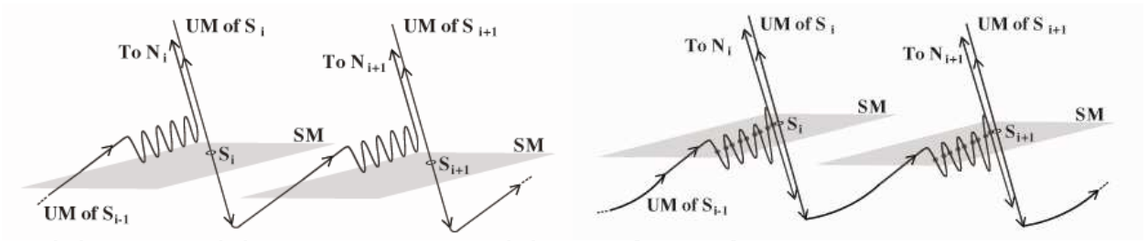

(a) $\alpha < \alpha_{c1}$ ($\alpha \doteqdot \alpha_{c1}$) (b) $\alpha_{c1} < \alpha < \alpha_{c2}$

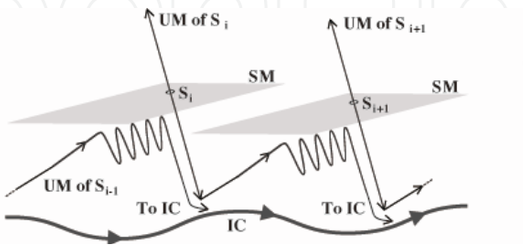

(c) $\alpha > \alpha_{c2}$($\alpha \doteqdot \alpha_{c2}$)

Fig. 7. A schematic diagram of the behavior of UM and SM around the bifurcation point. The stable direction of S_i (SM) denotes 10 dimensional subspace and the unstable direction of S_i denotes 1 dimensional curve.

becomes a saddle of index 1 and the corresponding saddle is an index 2 saddle. On the other hand, at the PF point two saddles appear in the backward direction as shown in Fig.6(a); namely, this is the subcritical PF bifurcation. Figure 6 (b) presents the 3D schematic diagram for better understanding the behavior of stable and unstable manifold of saddles in Fig.7. Here the stable direction denotes 10 dimensional subspace and the unstable direction denotes 1 dimensional curve[6].

Due to Kuznetsov (Kuznetsov; 1995), there exist many heteroclinic points formed by UM of S_i, S_i' (one dimensional in this case) and stable manifold (SM) of S_{i+1}, S_{i+1}' (ten dimensional in this case) around the bifurcation point for $\alpha_{c1} < \alpha < \alpha_{c2}$. Figures 7 (a), (b) and (c) present the schematic diagrams representing the connection of S_i,N_i, i = 1, 2, … ,6 for $\alpha < \alpha_{c1}$, $\alpha_{c1} < \alpha < \alpha_{c2}$, and $\alpha_{c2} < \alpha$. The UM of S_i waves severely as it approaches the SM of S_{i+1} for all cases. For $\alpha < \alpha_{c1}$, as seen in Fig.7 (a), UM of S_i finally converges to N_{i+1}. The UM and SM do not intersect. Therefore, a stable node corresponding to the periodic solution appears. For α much smaller than α_{c1}, the UM emanating from S_i goes to N_{i+1} directly without approaching near S_{i+1}. For $\alpha_{c2} < \alpha$, as seen in Fig.7 (c), UM of S_i eventually converges to invariant curve (= IC). The IC is the *propagating pulse wave just after birth* going left or right as shown in Fig.2. The UM also has no intersection with the SM. For α much larger than α_{c2}, the UM emanating from S_i goes to the IC without undulating near S_{i+1}. For $\alpha_{c1} < \alpha < \alpha_{c2}$, as seen in Fig.7 (b), UM of S_i goes two directions. The UM of S_i and SM of S_{i+1} intersect transversally. At $\alpha = \alpha_{c1}$, α_{c2}, the heteroclinic tangency occurs; namely, UM is tangent to SM.

[6] For example, for $\varepsilon = 0.36$, $\beta = 3.2$, $\alpha = 0.0883$, the eigenvalues of the saddles S_i and S_i' are as follows: 1.010, 0.925, 0.547, 0.402 ± 0.073*i*, 0.398, 0.345 ± 0.107*i*, 0.319 ± 0.164*i* and 0.142.

To clarify the above, we perform computer simulation in Fig.8 (a), (b) and (c)[7]. The UM can be presented in two dimensional phase space, because it is one dimensional. However, the SM cannot be presented in two dimensional phase space, because it is ten dimensional. Fortunately, the dominant eigenvalue of SM is 0.925 only and other nine eigenvalues are much smaller than unity as previously mentioned in the footnote. Therefore, we draw the stable eigenvector associated with this eigenvalue by the thick line for reference. Figure 8 (a), (b) and (c) demonstrate 3 cases. The waving thin curve presents the UM of S5. Since we cannot show whole ten dimensional stable manifold, we cannot obtain the critical values α_{c1}, α_{c2} from the figures. Therefore, we estimate whether or not the given α is within $\alpha_{c1} < \alpha < \alpha_{c2}$, by knowing the destination of UM. Namely, if it converges to N6, the given α is smaller than α_{c1}, and if it converges to IC, the given α is greater than α_{c2}, and if it is separated in two directions, the given α is in between α_{c1} and α_{c2}. In Fig.8 (a) the UM goes to N6. Therefore, in this case $\alpha < \alpha_{c1}$. In Fig.8 (b) UM of S_5 is separated in two directions along the UM of S_6, therefore, α is set between $\alpha_{c1} < \alpha < \alpha_{c2}$. In Fig.8 (c) UM goes to IC, therefore, α is set for $\alpha_{c2} < \alpha$.

In the same manner, the connection between S'_i and N_i, i = 1, 2, … ,6 can be explained in the following. For $\alpha < \alpha_{c1}$, the UM of S'_i goes to N_{i-1}. For $\alpha_{c1} < \alpha < \alpha_{c2}$, the UM of S'_i and SM of S'_{i-1} intersect transversally. For $\alpha_{c2} < \alpha$, the UM of S'_i eventually converges to the IC corresponding to the propagating pulse wave just after birth. Therefore, the propagating direction depends on the initial condition.

Since α_{c1} and α_{c2} are very close, we recognize them as the same number: $\alpha_c = \alpha_{c1} = \alpha_{c2}$ = 0.088302 for convenience. In addition, α_c (=0.088302) and α_{PF} (=0.088328) are close to α_{SN} (= 0.088501), therefore we say that the propagating pulse wave occurs at the SN bifurcation point approximately. For other values of β in $3.14 \leqq \beta \leqq 3.25$, we confirmed the same bifurcation structure ensuring generation of IC. For $\beta \geqq 3.26$ and $\alpha > \alpha_{PF}$ ($\fallingdotseq \alpha_{SN}$), one of the UM of each saddle goes to the stable node representing the whole oscillation (W in Fig.5). For $\beta \leqq 3.14$ and $\alpha > \alpha_{PF}$ ($\fallingdotseq \alpha_{SN}$), it goes to the stable node representing the zero solution (Z in Fig.5).

Practically, for $3.14 \leqq \beta \leqq 3.25$, if the initial condition is set on the periodic solution (standing wave solution) and increase α, the periodic solution persists up to $\alpha = \alpha_{PF}$ and for $\alpha > \alpha_{PF}$, the periodic solution jumps to the propagating wave solution (IC). On the contrary, if the initial condition is set on IC for $\alpha > \alpha_{PF}$ and then decrease α, the IC disappears at $\alpha = \alpha_c$ to become the periodic solution (standing wave solution). Namely, a hysteresis phenomenon between the standing wave solution and the propagating wave solution can be seen in $\alpha_c \leqq \alpha \leqq \alpha_{PF}$.

4. Conclusions

In this chapter, we revealed existence of the propagating wave in the ring of coupled bistable oscillator system. Then, we give one of the onset mechanisms of the propagating

[7] The shape of UM is obtained, together with the compensation algorithm, by repeating the mapping of which initial value is chosen on the unstable eigenvector(Parker & Chua; 1989). The method to obtain initial point on the unstable eigenvector is referred to (57) in (Katsuta & Kawakami; 1993). Numerical integrations for the compensation algorithm are carried out with 4th order Runge-Kutta method with step size = 0.001.

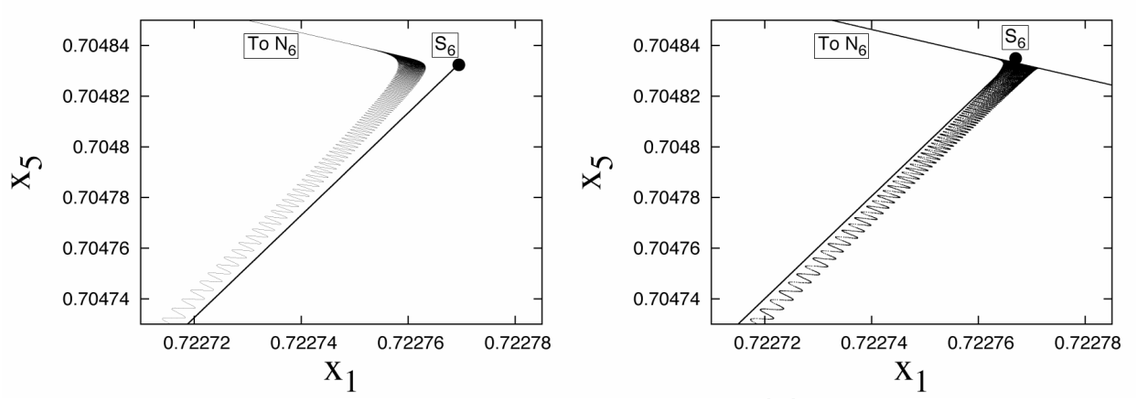

(a) $\alpha = 0.088302850$ (b) $\alpha = 0.088302864$

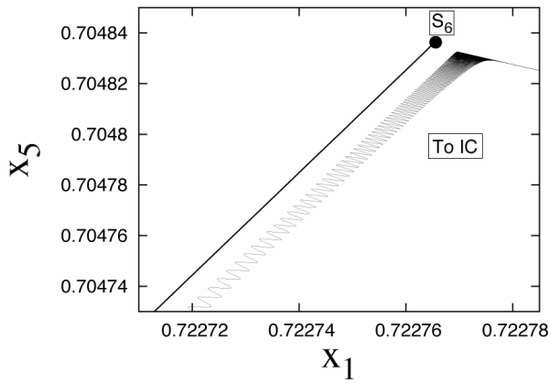

(c) $\alpha = 0.088302872$

Fig. 8. Three situation of UM of S_5 (thin curve) and a stable eigenvector of S_6 (thick line) corresponding to the largest stable eigenvalue.

pulse wave for the ring of 6 coupled bistable oscillators by exploring global phase-space structure around the bifurcation point. The transition from the standing pulse wave to the propagating pulse wave is due to the heteroclinic tangle shown in Fig.7. In our forthcoming paper, we will investigate these subjects more in detail.

5. References

Y. Nishiura, D. Ueyama and T. Yanagita, "Chaotic pulses for discrete reaction diffusion systems", SIAM J. Applied Dynamical Systems, vol.4, no.3, pp.723-754, 2005.

J.C. Comte, S. Morfu and P.Marqui´e, "Propagation failure in discrete bistable reactiondiffusion systems: Theory and experiments", Phys. Rev. E, vol.64, 027102, 2001.

K. Kaneko, "Chaotic traveling waves in a coupled map lattice", Phyisica D, vol.68, pp.299-317, 1993.

T.Hikihara, K.Torii and Y.Ueda, "Wave and basin structure in spatially coupled magnetoelastic beam system -Transitions between coexisting wave solutions", Int. Journal of Bifurcation and Chaos, vol.11, no.4, pp.999-1018, 2001.

M. Yamauchi, M. Wada, Y. Nishio and A. Ushida, "Wave propagation phenomena of phase states in oscillators coupled by inductors as a ladder", IEICE Trans.Fundamentals, vol.E82-A, no.11, pp.2592-2598, 1999.

M.Sato, B.E.Hubbard, A.J.Sievers, B.Ilic, D.A.Czaplewski and H.G.Craighead, "Observation of locked intrinsic localized vibrational modes in a micromechanical oscillator array", Phys.Rev.Lett., vol.90, no.4 (2003) 044102.

J.P. Keener, "Propagation and its failure in coupled systems of discrete excitable cells", SIAM J. Appl. Biol., vol.47, no.3, pp.556-572, 1987.

K.Shimizu, T. Endo and D.Ueyama, "Pulse Wave Propagation in a Large Number of Coupled Bistable Oscillators", IEICE Trans. Fundamentals, vol.E91-A, no.9, pp.2540-2545, 2008.

T. Endo and T. Ohta, "Multimode oscillations in a coupled oscillator system with fifthpower nonlinear characteristics", IEEE Trans. on circuit and systems, vol.cas-27, no.4, pp.277-283, 1980.

T. Yoshinaga and H. Kawakami, "Synchronized quasi-periodic oscillations in a ring of coupled oscillators with hard characteristics", Electronics and Communications in Japan, Part III, vol.76, no.5, pp.110-120, 1993.

H. Kawakami, "Bifurcation of periodic responses in forced dynamic nonlinear circuits: computation of bifurcation values of the system parameters", IEEE Trans. Circuits Syst., vol.CAS-31, no.3, pp.248-260, 1984.

T.S.Parker and L.O.Chua, Practical numerical algorithms for chaotic systems, Springer-Verlag, New York, 1989.

Y. Katsuta, H. Kawakami, "Bifurcations of equilibriums and periodic solutions in nonlinear autonomous system with symmetry", Electronics and Communications in Japan, Part III, vol.76, no.7, pp.1-14, 1993.

Y.A. Kuznetsov, "Elements of applied bifurcation theory", Springer-Verlag, New York, p.466, 1995.

A. The propagating pulse wave PW2

The PW2 is a certain kind of propagating pulse wave. The mapped points of PW1 and PW2 projected onto the (x_1, x_3, x_5) phase space are shown in Fig.9(a) and (b), respectively. Comparing both cases, each flow on the phase space moves along a different orbit. In addition, for PW1 the mapped points stay for a long time on several points (which correspond to the locus of the nodes N_i, i = 1, 2, … , 6.). This is one of characteristic feature of PW1 originating in the heteroclinic tangle. On the other hand, for PW2 the mapped points no longer stay the locus for a long time. Therefore, we distinguish PW2 from PW1. The existence region of such solution is shown in Fig.5. It should be noted that the starting point of PW2 is no longer close to the existence region of PS. That is, between them the existence region of W is sandwiched. For example, for β = 3.26 and ε = 0.36, PS disappears via PF bifurcation at $\alpha_{PF} \fallingdotseq 0.083$. In contrast, PW2 begins to exist for $\alpha \geqq 0.087$. Namely, there exists a gap between them. Probably, it originates in the standing wave where two adjacent oscillators are oscillating and where other oscillators are not. This is confirmed by continuously changing the parameter β of Fig.9. Further research will be necessary to clarify the generation mechanism of PW2.

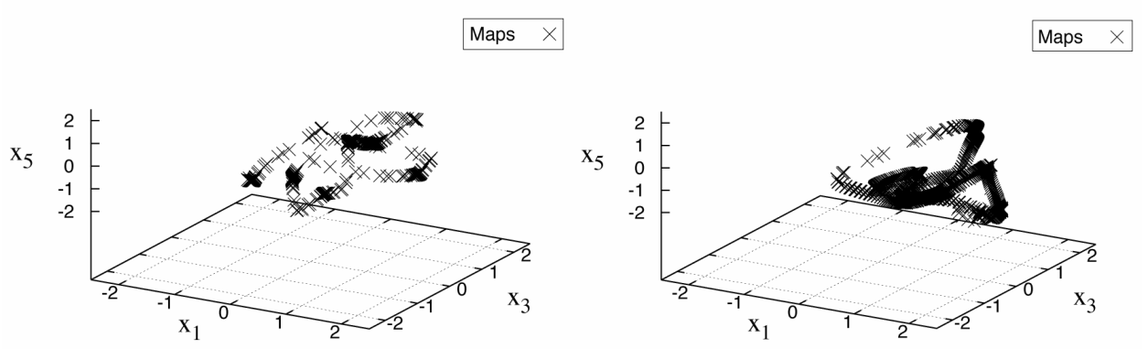

(a) Mapped points of PW1 (b) Mapped points of PW2

Fig. 9. Mapped points of PW1 and PW2 projected onto the (x_1, x_3, x_5) phase space. (a) PW1 (α = 0.089, β = 3.25 and ε = 0.36). The initial condition is given as x_1 = 2.0, y_2 = 1.3 and all other variables are zero. (b) PW2 (α = 0.089, β = 3.26 and ε = 0.36). The initial condition is given as x_1 = 1.7, x_2 = –2.2, x_3 = 0.9, x_4 = 0.2, x_5 = 0.1, x_6 = 0.5, y_1 = 1.8, y_2 = 0.4, y_3 = –2.3, y_4 = y_5 = 0.3 and y_6 = –0.3.

Wave Propagation in Materials for Modern Applications

Edited by Andrey Petrin

ISBN 978-953-7619-65-7
Hard cover, 526 pages
Publisher InTech
Published online 01, January, 2010
Published in print edition January, 2010

In the recent decades, there has been a growing interest in micro- and nanotechnology. The advances in nanotechnology give rise to new applications and new types of materials with unique electromagnetic and mechanical properties. This book is devoted to the modern methods in electrodynamics and acoustics, which have been developed to describe wave propagation in these modern materials and nanodevices. The book consists of original works of leading scientists in the field of wave propagation who produced new theoretical and experimental methods in the research field and obtained new and important results. The first part of the book consists of chapters with general mathematical methods and approaches to the problem of wave propagation. A special attention is attracted to the advanced numerical methods fruitfully applied in the field of wave propagation. The second part of the book is devoted to the problems of wave propagation in newly developed metamaterials, micro- and nanostructures and porous media. In this part the interested reader will find important and fundamental results on electromagnetic wave propagation in media with negative refraction index and electromagnetic imaging in devices based on the materials. The third part of the book is devoted to the problems of wave propagation in elastic and piezoelectric media. In the fourth part, the works on the problems of wave propagation in plasma are collected. The fifth, sixth and seventh parts are devoted to the problems of wave propagation in media with chemical reactions, in nonlinear and disperse media, respectively. And finally, in the eighth part of the book some experimental methods in wave propagations are considered. It is necessary to emphasize that this book is not a textbook. It is important that the results combined in it are taken “from the desks of researchers“. Therefore, I am sure that in this book the interested and actively working readers (scientists, engineers and students) will find many interesting results and new ideas.

How to reference

In order to correctly reference this scholarly work, feel free to copy and paste the following:

Kuniyasu Shimizu, Motomasa Komuro and Tetsuro Endo (2010). Pulse Wave Propagation in Bistable Oscillator Array, Wave Propagation in Materials for Modern Applications, Andrey Petrin (Ed.), ISBN: 978-953-7619-65-7, InTech, Available from: http://www.intechopen.com/books/wave-propagation-in-materials-for-modern-applications/pulse-wave-propagation-in-bistable-oscillator-array

INTECH
open science | open minds

InTech Europe
University Campus STeP Ri

InTech China
Unit 405, Office Block, Hotel Equatorial Shanghai

Slavka Krautzeka 83/A
51000 Rijeka, Croatia
Phone: +385 (51) 770 447
Fax: +385 (51) 686 166
www.intechopen.com

No.65, Yan An Road (West), Shanghai, 200040, China
中国上海市延安西路65号上海国际贵都大饭店办公楼405单元
Phone: +86-21-62489820
Fax: +86-21-62489821

IntechOpen

IntechOpen